STRUCTURAL, MORPHOLOGICAL AND OPTICAL CHARACTERIZATIONS OF ANNEALED EDTA CAPPED ZNS NANOCRYSTALS PREPARED BY CHEMICAL PRECIPITATION METHOD

M. A. Osman[1], A. A. Othman[1], Waleed A. El-Said[2], A. A. Abu-sehly[1], A. G. Abed-Elrahim[1]

[1] Physics and [2] Chemistry departments, Faculty of Science, Assiut University

Abstract

ZnS nanocrystals were prepared by the chemical co-precipitation method. The effect of annealing temperature (T_a) on the morphological**,** structural and optical absorption behavior was investigated using x-ray diffraction (XRD), high resolution transmission electron microscope (HRTEM), UV-vis spectroscopy, selected area electron diffraction (SAED) and Fourier transform infrared (FTIR) spectroscopy. Analysis of XRD patterns for as prepared and annealed samples showed that, increasing T_a leads to an increase in the crystallite size (D) from 2.67 to 19.6 nm. It is noticed that the obtained values of lattice parameters from HRTEM Images and SAED patterns are in good agreement with that deduced from XRD analysis. Furthermore, annealing process at 600 ^oC and 700 ^oC results, in complete phase transformation from as prepared ZnS cubic structure to ZnO hexagonal structure. Analysis of the XRD patterns, SAED, HRTEM and FTIR confirm this phase transition. Analysis of the optical absorption spectra indicates noticeable decrease in the direct band gap E_g^{opt} from 4.70 to 3.22 eV with increasing T_a. This behavior is attributed to the enhancement in crystallinity and the increase in particle size of ZnS nanoparticles. Moreover, UV photo-induced effect on the optical absorption edge was studied.

Keywords: annealing and UV induced effects, morphology, nanostructure, ZnS phase transition, optical absorption behavior

1. INTRODUCTION

In recent years, studies on semiconductor nanocrystals such as ZnS and CdS have drawn significant attention due to their unique structural, electronic and optical properties originating from their large surface to volume ratio and quantum confinement effect [1]. Usually the absence of appropriate stabilizer results in the reactivity and agglomeration of semiconductor nanoparticles [2]. ZnS is a promising material for various device applications such as electroluminescence devices [3], field emission displays [4] and sensors [5,6], light emitting diodes in the near UV region [7]. Considerable effort has been paid to tune properties of ZnS nanoparticles such as optical band gap, electronic structure and luminescence properties by changing their particle size. The thermal annealing process results in remarkable changes in the structure, absorption edges due to the movement of dislocations, native defects and adsorption / decomposition on the surface. In this study nanoparticles of ZnS capped with EDTA were prepared by the chemical co-precipitation method. Thermal annealing effects on morphological, structural and optical properties have been studied. In addition UV induced effect on optical absorption edge was investigated.

2. EXPERIMENTAL DETAILS

2.1. Sample preparation

ZnS nanoparticles were synthesized at room temperature using the chemical precipitation method. Zinc acetate ($Zn(CH_3COO)_2$) and sodium sulfide (Na_2S) were used as source materials and EDTA ($C_{10}H_{16}N_2O_8$) as a capping agent. All chemicals used were of AR grade. 0.8 M $Zn(CH3COO)_2.2H_2o$ was dissolved in 75 ml double distilled water, 0.08 M EDTA was added to solution of Zn^{+2} ions as capping agent and 0.8 M of Na_2S was dissolved in

75 ml double distilled water and added drop wise at fixing stirring 400 rpm. The obtained fine white precipitate was filtered out and washed several times with distilled water and ethanol to remove unnecessary impurities formed during the preparation process. ZnS samples were dried at 100 °C for 3 hrs to remove moisture. To study the effect of annealing process on morphological, structural and optical properties, the samples of ZnS were annealed in the temperature range 125–700 °C in atmospheric air with the step of 100 °C, then the samples were cooled to room temperature at the rate of 10 °C/min.

2.2. Characterization

The Crystal structure of ZnS nanoparticles was characterized by X-ray diffraction (PW 1700 X-ray diffractometer with Cu Kα radiation λ=1.54056Å). Diffraction patterns were recorded in the range of the diffraction angle 2θ from 20° to 70° with a step of 0. 06°. UV-vis optical absorption spectra were studied using Perkin Elmer lambda 750 spectrophotometer at room temperature. Fourier transform infrared spectroscopy (FTIR) [Nicolet™ iS™10 FTIR Spectrometer] was used to identify the functional groups in the samples. Particle size, morphology and crystalline nature were investigated by using HRTEM [Jeol Jem 2100 microscope operating at 200 kV]. UV induced effect was studied by using mercury lamp [VL-6.LC] at λ =254 nm and power of 6 watt.

3. RESULTS AND DISCUSSION

3.1. XRD analysis

The structure of the as prepared and annealed samples of ZnS nanoparticles was characterized using x-ray powder diffraction. Fig. 1(a) shows that, XRD pattern for as prepared sample exhibits three diffraction peaks at 2θ values of 28.34°, 47.48° and 56.12°, which match perfectly with the (111), (220) and (311) crystalline planes of ZnS cubic phase with standard card [JCPDS:04-012-7581]. The peak broadening in the XRD patterns indicates the nanocrystalline nature of the samples. The average particle size (D) of the as prepared and annealed samples of ZnS nanocrystallites is estimated by using Debye Scherer's formula [8]:

$$D = \frac{K\lambda}{\beta \cos\theta} \quad (1)$$

Which, $K \cong 0.9$ is the particle shape factor, the x-ray wavelength λ = 0.154nm, β is the full width at half-maximum intensity (FWHM), θ is the Bragg angle in degrees. According to the above equation, the average crystallite size (D) of the as prepared ZnS nanocrystallites was 2.67nm. In the temperature range 35°C-150°C D slightly decreases accompanied by remarkable increase in E_g^{opt} due to the capping effect. Furthermore, it has been observed that increase in T_a from 150°C to 700°C leads to an increase in D, accompanied by decrease in the internal local strain (ε) which is deduced from the following equation [9]:

$$\frac{\beta \cos\theta}{\lambda} = \frac{1}{D} + \frac{4\varepsilon \sin\theta}{\lambda} \quad (2)$$

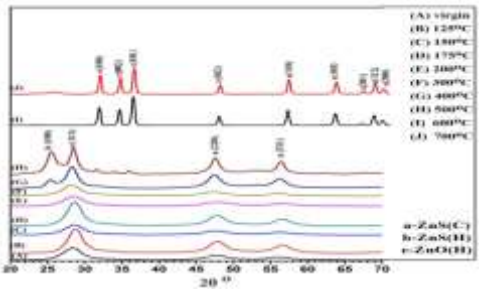

Fig. 1(a) XRD patterns of ZnS nanoparticles at different annealing temperatures

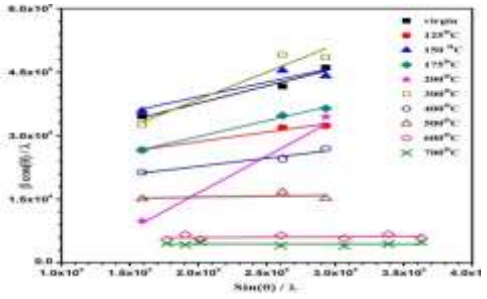

Fig. 1(b) Plot of $\beta\cos\theta/\lambda$ vs. $\sin\theta/\lambda$ of ZnS nanoparticles at different annealing temperatures.

Fig. 1(b) shows the plot of $\beta \cos\theta / \lambda$ versus $\sin\theta / \lambda$ for ZnS. (ε) was determined from the slope of the straight line. The results of XRD, SAED patterns and HRTEM images are given in table 1. The lattice parameters and d_{hkl} for all phases at 400°C and 500°C reveal good agreement with these values of ZnS and ZnO bulk crystals. The percentage of all phases has been estimated based on the integrated intensity of the diffraction peaks. Moreover, in the presence of air at T_a = 600 °C, the mixed phases of ZnS were converted completely into ZnO hexagonal phase [10]. The average particles size of ZnO was found to be 14.8 nm. Furthermore, with increasing T_a up to 700 °C, D increases to 19.6 nm, and was associated with enhancement in crystallinity. The phase transition of ZnS into ZnO can be explained as follows: 1) Oxidation of ZnS takes place during annealing process in the ambient air via the exchange reaction between oxygen and sulfur according to the following equation [11]: $2ZnS + 3O_2 \xrightarrow{600oC} 2ZnO + 2SO_2 \uparrow$ (3)

2) Formation of ZnO hexagonal phase as a result of sulfur sublimation as H_2S due to thermally assisted chemical decomposition of hydroxyl group. From our point of view the first reason is the most probable. Moreover, the above interpretation is confirmed by FTIR spectral analysis.

3.2. FTIR analysis

Fig. 2(a) show the FTIR spectrum of the as prepared ZnS, which demonstrates a strong sharp peak at 1632 cm^{-1}, which could be attributed to the carbonyl (stretching C=O) group and stretching peak at 3426cm^{-1} for OH group. In addition, vibration peaks at 561cm^{-1} (asymmetric bending), and 671cm^{-1} (symmetric bending) are attributed to stretching vibrations of Zn-S bonds.

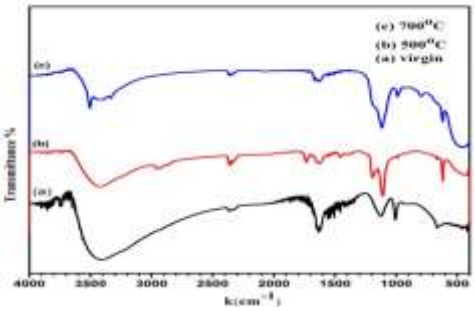

Fig. 2 FTIR spectra for as prepared ZnS and annealed samples at T_a= 500 °C and 700 °C

FTIR spectrum of the pre-treated ZnS nanoparticles at 500 °C (fig. 2(b)) reveals a broad vibration at 3441 cm^{-1} (due to stretching vibrations O-H bond), which confirmes the presence of moisture on the surface of ZnS nanostructures. Furthermore, fig. 2(c) shows the FTIR spectrum of ZnS nanoparticles after annealing at 700 °C for 3 hrs, indicates the appearance of new vibration peak at 433cm^{-1} that could be assigned to the ZnO stretching and the disappearance of two vibration peaks at 561 cm^{-1} and 671 cm^{-1} (ZnS). These results indicate that the annealing of ZnS nanoparticles for 3hrs results in, the oxidation of ZnS and the formation of ZnO.

3.3. Optical absorption characteristics

3.3.1 Annealing effect

Fig. 3(a) shows the Optical absorption spectra of the as prepared and annealed samples of ZnS nanoparticles. It is observed that the absorption inset lies below 300 nm. In the temperature range from 35 °C to 300 °C, these spectra reveal an excitonic absorption shoulder at about 310 nm due to strong quantum size effect, where the average particle size (2.6 - 2.8nm) is smaller than the Bohr exciton radius ~ 3 nm of ZnS. Further increase of annealing temperature results in an increase in the exciton absorption, without any change in its position. Similar excitonic absorption peak was observed in ZnS and CdS nanocrystals at 300 nm and 314 nm respectively [12]. The optical band gap E_g^{opt} was determined by using Tauc relation [13]:

$(\alpha h\nu) = B\,(h\nu - E_g^{opt})^{n}$ (4)

Where $n = 1/2$ for the direct allowed transition α is the absorption coefficient, hv is the photon energy and B is the steepness parameter. The plots of $(\alpha h\nu)^2$ vs. hv at different annealing temperatures are given in fig. 3(b). The values of E_g^{opt} are given in table (1). In the temperature range 35 °C-150 °C the particle size exhibit a slight decreasing accompanied by a remarkable increasing in E_g^{opt} (i.e blue shift). Moreover, it is noticed that E_g^{opt} of annealed samples below 400 °C is greater than ~ 3.6eV for bulk ZnS [14, 7]. This blue shift is attributed to the quantum size effects of ZnS nanoparticles [15, 16]. In addition, increase in T_a from 150 °C to 500 °C results, in remarkable increase in D accompanied by red shift in the absorption edge. The disappearance of exciton shoulder at 400 °C and 500 °C may be ascribed to one or both of the following reasons:(1) when the particle size increases the quantum confinement of electrons and holes decreases, consequently, both the overlap factor between their wave functions and the absorption cross-section decrease, this results in disappearance of exciton peak.

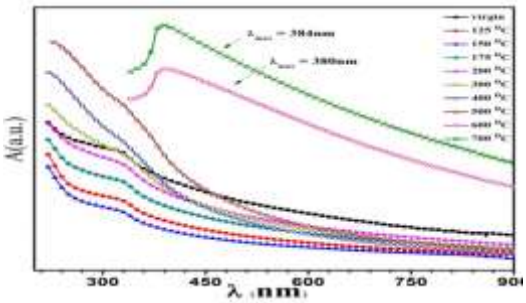

Fig. 3(a) Optical absorption spectra for as prepared and annealed samples of ZnS nanoparticles at different T_a

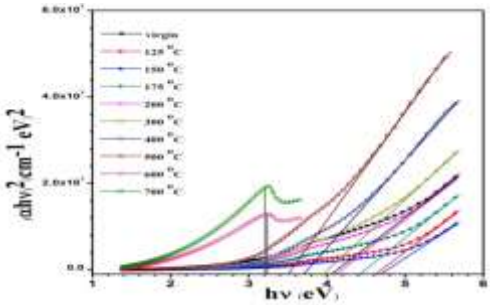

Fig. 3(b) plots of $(\alpha h\nu)^2$ versus hv at different T_a, the inset represents dependence of E_g^{opt} and D on T_a

(2) The presence of trapping centers for electrons and holes due to surface defects within the energy gap results in strong interaction between the trapped electron–hole pair and exciton and hence bleaching of exciton absorption [17]. Furthermore, from the blue shift of the band gap values $\Delta E_g^{opt} = E_g^{opt}(\text{nano}) - E_g^{opt}(\text{bulk})$, the average particle size D was calculated using the brus equation [18, 19]:

$$E_g^{opt}(\text{nano}) - E_g^{opt}(\text{bulk}) = \frac{\hbar^2\pi^2}{2D^2}\left(\frac{1}{m^*_h} + \frac{1}{m^*_e}\right) - \frac{1.8\,e^2}{4\pi\epsilon_0\epsilon_r D} \quad (5)$$

where $E_g^{opt}(\text{nano})$ and $E_g^{opt}(\text{bulk}) \cong (3.6\text{eV})$ are the optical band gap of nano and bulk ZnS semiconductor [20,21]), m^*_e and m^*_h are the effective masses of electron and hole respectively, ϵ_r is the relative dielectric constant, ϵ_0 is the permittivity of free space. The obtained values of D are listed in table (1). In a strong confinement as in the present case, the second term is small and may be neglected [22].

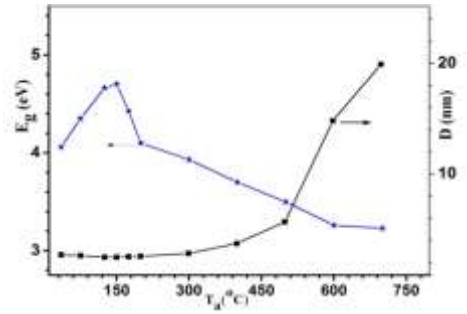

Fig. 3(c) Dependence of E_g^{opt} and D on annealing temperatures

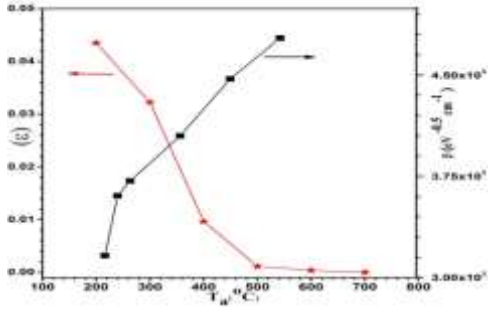

Fig. 4 Dependence of steepness parameter (B) and internal lattice strain (ε) on annealing temperatures

As a result of the annealing process both the degree of crystallinity and particle size increase, hence E_g^{opt} decreases [fig. 3(c)]. The overall decrease in E_g^{opt} may be ascribed to one or more of the following reasons: (1) the reduction in the density of surface defects and dangling bonds on the surface of ZnS nanoparticles via

the annealing process. At T_a = 500°C, HRTEM image in fig. 8(b) reveals small number and large size of domains with different orientations. This observation together with SAED confirms enhancement in crystallinity. (2) Reduction of the tail states width which can be ascribed to reduction of structure and surface defects which are localized on the domain boundaries accompanied with the increase in ordering parameter B as shown fig. 4, which indicates the enhancement in crystallinity.

3.3.2. UV induced effect

Fig. 5(a, b) show tauc analysis for optical absorption of ZnS dispersed in double distilled water, which irradiated by UV photons at different times in the range from 0 to 120

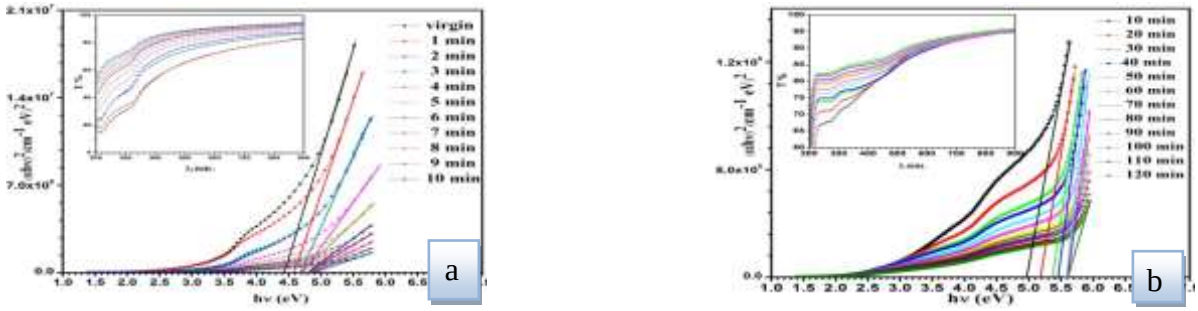

Fig. 5(a, b) $(\alpha h\nu)^2$ vs. hv of ZnS nanoparticles at different UV irradiation times τ and T% vs. λ on the inset

The Increase in UV irradiation times results, in enhancement of transmittance spectrum (photo-bleaching) [fig. 5(a,b)], accompanied by increase in E_g^{opt}. This behavior can be explained in terms of two stages process stimulated by optical excitation: (a) photoionization which occur essentially due to Auger process, in which one electron – hole pair recombine providing an extra electron energy to leave the crystallite. (b) Stimulated photolysis providng an irreversible corrosion i.e. reduction of particle size, which leads to stronger overlap between electron and hole wave function, hence enhancement of transmittance and increase E_g^{opt}[23]. Photoionization induces sequence of chemical reactions by means of Auger process yield an excess electron outside the crystallite and an excess hole inside or at the surface that is can be expressed simialr to those reported for CdS by Henglein [24]:

$$(ZnS)_n \xrightarrow{h\nu} (ZnS)_n(e^- + h^+) \xrightarrow{h\nu} (CdS)_n(e^- + h^+)_2 \longrightarrow (ZnS)_n(h^+) + e^- . \quad (6)$$

After photoionization, the remaining hole may act an oxdizing agent and itiate the secondary chemical reactions at the ZnS surface i.e photo passivation. Sulfide anions can be oxidized to the radical anion S^- by h^+ with further oxidation by air oxygen SO_2^- or SO_4^- that is , $h^+ + S^{-2} \longrightarrow S^-$, $S^- + O_2 \longrightarrow SO_2^- \xrightarrow{O2} SO_4^{-2}$ (7)

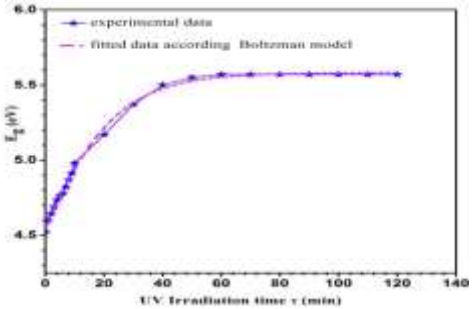

Fig. 6 dependence of E_g^{opt} on UV irradiation timeτ

Such anions have been detected after photolysis of CdS nanoparticles colloidal solution by Kamat [25]. Fig. 6 shows the dependence of E_g^{opt} on UV irradiation times (τ) which obey an empirical equation in a good agreement with Boltzmann fitting for our data, with adjusting R^2 = 0.998 as follow:

$$E_g^{opt} = 5.58 - \frac{2.787}{e^{(\frac{\tau+7.876}{14.74})}} \quad (8)$$

It is observed that two characteristic regions of E_g^{opt} dependence on UV irradiation time τ . First region from the start of UV exposing up to nearly 40 minute, the second from 40 minute up to 120 minute. We suggest that, in the first region, photolysis stimulated by photo ionization of nanoparticles is more prominent, consequently rapid decrease in the corresponding dispersed particle size and enhancement of quantum size effect that leads to increasing of optical band gap and transmittance enhancement. Second region photo-oxidation is the most prominent, results, in photo-passivation on the surface of, Hence stability of particle size value, which reflect the saturation in E_g^{opt} with irradiation time at higher times

3.4. Morphological studies

The morphologies of ZnS nanoparticles have been investigated by using analysis of TEM images. Calculation of the mean value of particle size (D) was carried out by the statistical distribution method. Analysis of TEM image and the corresponding particle size distribution of the as prepared ZnS [fig. 7(a)], showed that, the particles are monodispersed (where standard dev. $\approx 3.5 <$ 7%) and exhibit narrow size distribution in the range 3 - 23 nm. TEM image indicates that ZnS nanoparticles exhibit nearly spherical shapes of different sizes. The large value of D (8.5 ± 3.5nm) can be ascribed to the aggregation process of small nanocrystallites to produce large agglomerates, as a result of moisture effects during preparation of ZnS for TEM studies. FTIR for as prepared sample confirms our point of view.

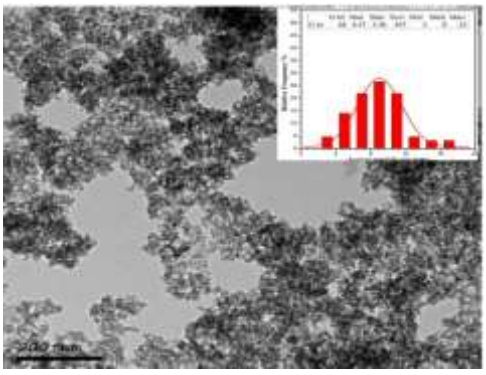

Fig. 7(a) TEM image of as prepared ZnS nanoparticles and histogram on the inset

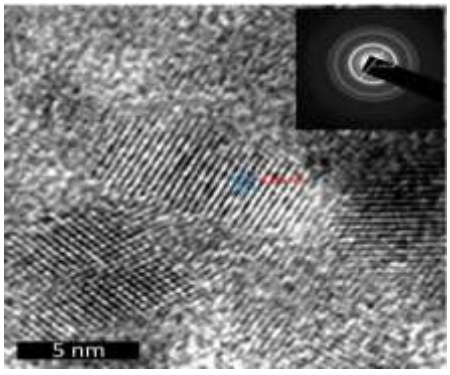

Fig. 7(b) HRTEM image and SAED for as prepared ZnS nanocrystallites

Fig. 7(b) indicates that, HRTEM image of the as prepared ZnS reveals a number of polycrystalline domains with distinct domain boundaries. The inset of fig. 7(b) represents SAED pattern for as prepared capped ZnS, it consists of three concentric intense and sharp diffraction rings, which demonstrate the polycrystalline nature of the cubic ZnS [26]. The lattice parameters and interplanar distances d_{hkl} of the cubic ZnS nanoparticles deduced from HRTEM image are consistent with that deduced from SAED, XRD as shown in table (1). TEM morphology at T_a = 500°C in fig. 8(a) reveals large domains (agglomerates) that consist of a nearly spherical and hexagonal shaped structure. From the corresponding histogram D = 19.7 ± 3.5 nm. The noticeable large average particle size deduced from TEM morphology as a result of the annealing process can be attributed to the following reasons: (1) Thermally assisted aggregation and flocculation of small nanocrystallites to produce large irregular agglomerates. This results in good agreement with that obtained by Kitamura [19]. (2) The reduction of structural defects which results in an increase in the crystallinity and decrease in the internal local strain (ε) associated with decreasing in the surface tension $\sigma = \sigma_{\infty} + \frac{Constant}{D}$, where σ_{∞} equals σ as $D \longrightarrow \infty$, therefore, the

particle size D increase [29]. Moreover, HRTEM image at 500°C fig. 8(b) reveals a smaller number of large polycrystalline domains rather than that observed for as prepared sample as a result of thermally assisted aggregation and emerging of domain. Hence as T_a increases domain boundary decreases, as well as two preferable orientations corresponding to the lattice parameters of ZnS cubic and hexagonal structure were observed. These results are in good agreement with standard cards [JCPDS:04-012-7581and 04-015-3042. XRD pattern show that the equilibrium temperature for the cubic to hexagonal transition in ZnS nanoparticles is 400°C which is significantly smaller than that of the bulk value (1020°C) [27-28].

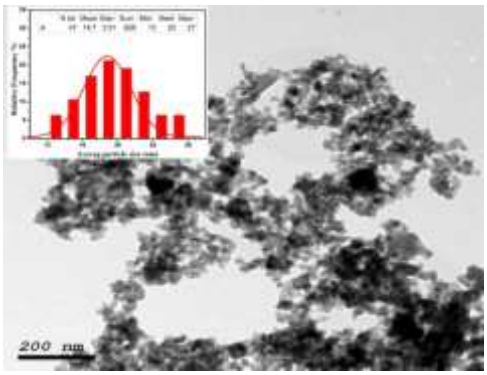

Fig. 8 (a) TEM image and the corresponding histogram of annealed ZnS at T_a = 500°C

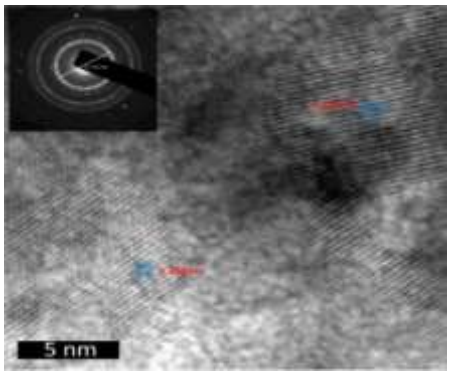

Fig. 8(b) HRTEM image and SAED for annealed ZnS at T_a = 500°C

HRTEM and SAED results confirm the existence of the two mixed phases at T_a = 500°C.results confirm the existence of the two mixed phases at T_a = 500°C. This behavior can be attributed to tendency of nanoparticles to move and aggregate easily, thereby increasing the average particle size. TEM morphology at T_a = 700°C as seen in fig. 9(a) exhibits large and single crystalline particles of ZnO, as a result of complete phase transition of as prepared polycrystalline domains of ZnS cubic phase to monocrystalline domain of ZnO hexagonal phase. These domains reveal a hexagonal-shape. It is found that, the mean particle size obtained from TEM higher than that deduced from Debye-Scherer equation [table (1)]. This discrepancy can be ascribed to one or more of the following reasons:(1)The particle size calculated from XRD data represent thickness averaged magnitude, which is usually dominated by the smallest crystallites [30].(2) TEM image demonstrates the surface features and give the maximum possible size of grains [31],since the nanocrystalline particles near the surface of ZnS domains have a tendency to increase its size via the annealing process.(3) The use of different detection techniques.(4) During sample preparation for HRTEM characterization, the smaller nanoparticles may physically merge and contact each other to form a larger particle size as a result of moisture effects [32].

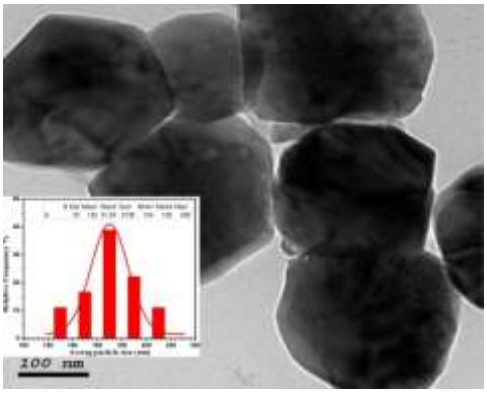

Fig. 9(a) TEM image of annealed sample at T_a = 700°C and the corresponding histogram on the inset

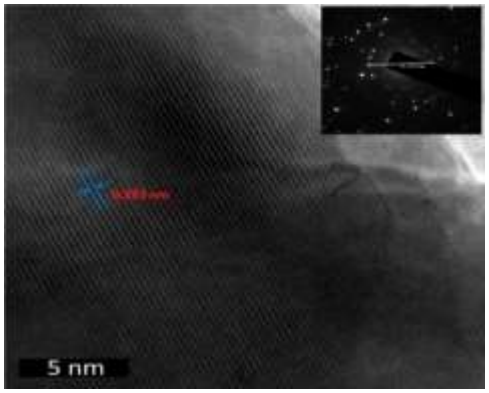

Fig.9 (b) HRTEM image and SAED for annealed ZnS nanoparticles at T_a = 700°C

Fig. 9(b) shows that, HRTEM at Ta =700°C reveals single crystalline domain where all lattice planes take the same preferable direction of orientation. Lattice parameters calculated from HRTEM image were in good agreement with XRD data and standard card (04-008-8199). Moreover, the SAED pattern indicates clearly bright and non uniform distribution of ZnO crystalline particles. Furthermore, HRTEM at T_a = 700°C exhibits single crystalline domain, where all the lattice planes take the same preferable direction of orientation. Lattice parameters calculated from HRTEM image were in good agreement with XRD data and standard card (04-008-8199). Moreover, the SAED pattern indicates clearly bright and non uniform distribution of ZnO crystalline particles.

Table (1): Dependence of D, E_g^{opt} d_{hkl} and lattice parameters of ZnS nanoparticles on the annealing temperatures.

T_a (°C)	Phase	Average particle size D (nm)			E_g^{opt} (eV)	H k l	Lattice parameters (Å)							
							Interplanar distance d_{hkl}				Average lattice constant a, b and c			
		TEM	XRD	Brus			XRD	HRTEM	SAED	Ref. card	XRD	HRTEM	SAED	Ref. card
as prepared	ZnS(C) 100%	8.5	2.67	2.45	4.06	(111)	3.125	3.15	3.154	3.12	a = b= c =5.406	a =5.456 b= 5.456 c =5.456	a =5.432 b= 5.432 c =5.432	a =5.411 b= 5.411 c =5.411
						(220)	1.90	—	1.86	1.913				
						(311)	1.637	—	1.68	1.632				
125		—	2.46	1.6	4.66	(111)	3.106	—	—	3.12	a = b = c = 5.380	—	—	
150		—	2.45	1.6	4.70		3.120	—	—		a = b = c =5.404	—	—	
175		—	2.51	1.8	4.43		3.108	—	—		a= b = c = 5.383	—	—	
200		—	2.54	2.3	4.10		3.127	—	—		a= b = c =5.416	—	—	
300		—	2.8	2.9	3.93		3.179	—	—		a=b = c = 5.510	—	—	
400	ZnS(C) 91%	—	3.7	5.2	3.7		3.146	—	—		a=b = c = 5.45	—	—	
	ZnS(H) 9%					(100)	3.500			3.310	—	—	—	—
500	ZnS(C) 66%	20	5.4	—	3.5	(111)	3.129	3.18	—-	3.120	a = b= c =5.41	a =5.5 b= 5.5 c =5.5	a =5.409 b= 5.409 c =5.409	a =5.411 b= 5.411 c =5.411
						(311)	1.630	—	1.6	1.632				
						(220)	1.910	—	1.93	1.913				
	ZnS(H) 26%					(100)	3.487	—	—	3.31	——	——	a =3.96 b= 3.96 c =12.3	a =3.827 b= 3.827 c=12.521
						(102)	—	3	—	2.930				
						(109)	—	—	1.27	1.283				
						(2010)	—	—	1	1.020				
	ZnO(H) 8%					(101)	2.49	—	2.46	2.460	a = b= 3.268 c =5.26	—	a =3.256 b= 3.256 c =5.2	a =3.251 b= 3.251 c =5.209
						(103)	—	—	1.48	1.482				
						(100)	2.83	—	—	2.820				
						(002)	2.63	—	—	2.600				
600	ZnO(H) 100%	—	14.8	—		(100)	2.823	—	—	2.820	a = b= 3.26 c =5.228	—	—	a =3.251 b= 3.251 c =5.209
						(002)	2.614	—	—	2.600				
700		152	19.6	—		(100)	2.813	2.83	—	2.830	a = b= 3.248 c =5.21	—	a =3.268 b= 3.268 c =5.238	a =3.251 b= 3.251 c =5.209
						(101)	2.475	—	2.45	2.49				
						(102)	1.91	—	1.93	1.912				
						(200)	1.41	—	1.43	1.41				
						(202)	-	—	1.24	1.238				

4. CONCLUSIONS

ZnS nanocrystals were prepared by chemical co-precipitation method. The samples were annealed in air for 3 h in steps of 100°C in the temperature range of 125–700°C. Phase change, lattice parameters, grain size has been deduced from XRD patterns, HRTEM and SAED. The main conclusions of the present work are:

(1) XRD analysis showed that, the equilibrium transition temperature for the cubic to hexagonal transition in ZnS nanoparticles starts at 400°C.(2) The absorption edge exhibits blue shift at T_a = 150°C ($E_g^{opt} = 4.7\ eV$), further increasing in T_a results in, an increase of the particle size accompanied by decrease in the optical band gap (red shift) from 4.7eV for ZnS cubic phase at 150°C to 3.22eV for the hexagonal phase of pure ZnO at T_a = 700°C.(3) HRTEM image at T_a = 700°C shows phase transition of the two mixed phases of ZnS and ZnO polycrystalline domains which appeared at 500°C to ZnO monocrystalline single-particle (4) Optical band gap, particle size and phase change were dependent on the annealing temperature, hence ZnS band gap can be tuned in the range 4.7 - 3.7eV via annealing process from 150°C to 400°C. (5) The annealing temperature 150°C is the more reasonable temperature for synthesizing of ZnS nanocrystallites. (6) UV irradiation of colloidal solution of ZnS nanoparticles leads to an enhancement in transmittance accompanied by increase in the optical band gap (photo brightening) as a result of photolysis and photo-passivation.

ACKNOWLEDGMENT

The authors would like to acknowledge the stuff members and assistances of nanotech-company for photo-electronics research for their technical help in HRTEM.

REFERENCES

[1] A. P. Alivisatos, Science 27 (1996) 933.
[2] M. N. Rittner, T. Abraham, Int. J. Powder Metall. 34 (1998) 33.
[3] T.Toyama,T. Hama, and D. Adachi, Nanotechnology, 20 (2009) 55203.
[4] S. H.Shin, J. H.Kang, D. Y.Jeon, and D. S.Zang, J. Solid State Chem, 178 (2005) 2205.
[5] Y. He, H. F. Wang and X. P Yan, Chem. Eur. J., 15 (2009) 5436.
[6] B. H.Dong, L. X.Cao, G. Su, W. Liu, H. Qu, and D. X.Jiang, J. Colloid. Interface Sci., 339 (2009) 78.
[7] Ni, Y., Yin, G., Hong, J., Xu, Z. Mater. Res. Bull., 39 (2004) 1967.
[8] K.K. Nanda, S.N. Sahu, Adv. Mater., 13 (2001) 280.
[9] Suryanarayana, C, Grant Norton, M: X-ray Diffraction: A Practical approach. springer, new York (1998).
[10] D.Amaranatha Reddy, G. Murali, B. Poornaprakash, R. P. Vijayalakshmi, and B. K. Reddy, Solid State Commun., 15 (2012) 596.
[11] Hao-Ying Lu, Sheng-Yuan Chu, Soon-Seng Tan, J. Cryst. Growth 269 (2004) 385.
[12] Rong He, Xue-feng Qian, Jie Yin, Hong-an Xi, Li-juan Bian, Zi-kang Zhu , Colloids Surf. A: Physico chem. Eng. Aspects 220 (2003) 151
[13] H.K. Yadav, K. Sreenivas, R.S. Katiyar, V. Gupta, J. Phys. D: Appl. Phys. 40 (2007) 6005.
[14] R. Pool, Science, 24 (1990) 1186.
[15] P. Prathap, N. Revathi, Y.P. Venkata Subbaiah, K.T. Ramakrishna Reddy, J. Phys. Condens. Matter 20 (2008) 035205.
[16] D.H. Kim, D.J. Lee, N.M. Kim, S.J. Lee, T.W. Kang, Y.D. Woo, D.J. Fu, J. Appl. Phys. 101(2007) 094111.
[17] Y.Wang, N. Herron, J. Phys. Chem., 95 (1991) 525.
[18] L.E. Brus, J. Phys. Chem , 90 (1986) 2555.
[19] Y. S. Yang, F. Y. Chen, Y. Y. Lee, C. L. Liu, Jan. J. Appl. Phys. 76 (1994) 304.
[20] YG .Wang, SP .Lau, HW. Lee, Yu SF, BK. Tay, XH. Zhang, et al. J. Appl. Phys. 94 (2003) 354.
[21] S. Dutta, M. Chakrabarti, S. Chattopadhyay, D. Jana, D. Sanyal, A.Sarkar, J Appl Phys 98 (2005) 053513.
[22] G. Ghosh, M. Kanti Naskar, A. Patra, M. Chatterjee, Opt. Mater 28 (2006) 1047.
[23] S. V. Gaponenko, optical properties of semiconductor nano crystals, Cambridge university press, 1998
[24] A. Henglein, small particle research: physicchemical properties of extremely small colloid metal and semiconductor particles. Chem. Rev. 89, 1989, 1861-73
[25] P. V. Kamat, Photochemistry on nonreactive (semiconductor) surface, Chem. Rev. 93, 1993: 267-300.
[26] S. Liu, H. Zhang, M. T . Swihart, Nanotechnology 20 (2009) 235603.
[27] S. B. Qadri, E. F. Skelton, D. Dinsmore, J. Yang, H. F. Gary, and B. R. RAtna, Phys. Rev.B, 60 (1999) 9191.
[28] N. Shanmugam, S. Cholan, N. Kannadsan, K. Sathishkumar, and G. Vruthagiri, J. of nanomaterials, Volume 2013, doi.10.1155/2013/351798.
[29] S. B. Qadri, E. F. Skelton, D. Hsu, A. D. Dinsmore, J. Yang, H. F. Gray, and B. R. Ratna, Phys. Rev. B. condensed matter and material physics, 60 (1999) 9191
[30] K.P. Acharya, J.R. Skuza, R.A. Lukaszew, C. Liyanage, B. Ullrich, J. Phys Condens. Matt.,19 (2007) 19622.
[31] G. Korotcenkov, A. Cornet, E. Rossinyol, J. Arbiol, V. Brinzari, Y. Blinov, Thin Solid Films, 471(2005) 310.
[32] N. Goswami and P. Sen., Journal of nanoparticles research, 9 (2007) 513